

Superparamagnetic limit of antiferromagnetic nanoparticles

Unai Atxitia,^{1,2,*} Tobias Birk,¹ Severin Selzer,¹ and Ulrich Nowak¹

¹*Department of Physics, University of Konstanz, D-78457 Konstanz, Germany*

²*Freie Universität Berlin, Fachbereich Physik, Arnimallee 14, 14195 Berlin, Germany*

(Dated: December 15, 2024)

Antiferromagnetic materials are in the focus of current research in magnetism because of their potential for applications in spintronics. As for ferromagnets, their magnetic stability in nanostructures will be limited by thermal excitations. Here, we investigate the superparamagnetic limit of antiferromagnetic nanoparticles theoretically, focusing on a comparison to the known properties of ferromagnetic particles. We find a drastically reduced thermal stability because of the exchange enhancement of the attempt frequencies and the effective damping during the antiferromagnetic switching process.

Recent advances in understanding and controlling antiferromagnetic materials have lead to an increasing interest in antiferromagnetic spintronics [1–7]. Possible advantages of spintronic devices based on antiferromagnetic materials include their lack of stray fields, which normally destroys mono-domain states and leads to an interaction between bit patterns, the low susceptibility to external fields and the rich choice of new materials, including a variety of antiferromagnetic insulators. Moreover, antiferromagnetic spin dynamics are found to be faster than those of ferromagnets [4, 8–10].

However, for many applications the size of magnetic structures will have to be scaled down to the nanometer regime, where, eventually, thermal excitations will reduce the stability of the magnetic state. Whereas thermal stability of ferromagnetic nanoparticles have been studied extensively in the past [11–17, and references therein], antiferromagnetic nanoparticles have been barely investigated [18–21]. In this letter we investigate the differences and similarities of the thermally induced magnetization dynamics in ferromagnetic and antiferromagnetic nanoparticles.

A macroscopic ferromagnet (FM) is normally in a demagnetized state, where the stray-field energy is minimized by a multi-domain state. Only below a certain length scale - the exchange length - the mono-domain state is energetically favorable. For an antiferromagnet (AFM) this argument does not hold because of the missing macroscopic stray field and long-range order can be expected for much larger particle sizes, limited probably only by defects in connection with the ordering kinetics. When further reducing the size of the sample, thermal excitation will lead to probabilistic switching events where even for a mono-domain particle different switching mechanisms can occur. Some of them, as e.g. curling [22], are, once again, energetically dominated by stray field energy and will not appear in an AFM, so that here only two switching modes should dominate at lower temperature, namely coherent rotation [23] and nucleation followed by domain wall propagation [24].

For small particle size individual magnetic moments rotate coherently minimizing the exchange energy while

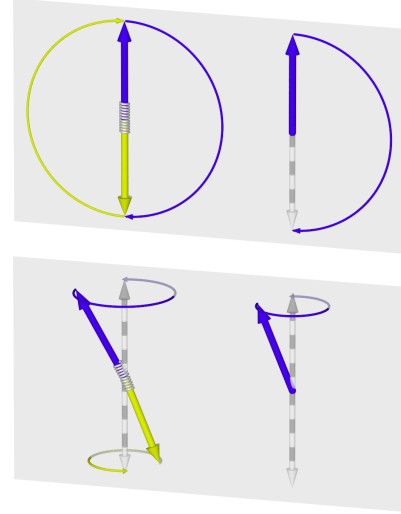


FIG. 1. Comparison of switching in FMs and AFMs: while the energy barriers for coherent rotation are identical the attempt frequencies strongly differ caused by the different dynamical properties of the FM and AFM eigenmodes.

overcoming the energy barrier that is due to the anisotropy of the system. With increasing system size nucleation must become energetically favorable since here the energy barrier is a constant, while it is proportional to the system size in the case of coherent rotation. For an elongated sample a critical length scale exists, $L_c = \pi\sqrt{2J/d_z}$, a value that is clearly related to the domain wall width $\delta = \sqrt{J/2d_z}$, where both are defined by the ratio between exchange J and anisotropy d_z energies. Above L_c , the nucleation of a pair of domain walls is energetically favorable as compared to the energy barrier, which has to be overcome by coherent rotation [22, 24–27]. Interestingly, these modes and the length scale separating the two modes, nucleation and coherent rotation, should be identical for FMs and AFMs, in so far as the concerned energies, the anisotropy energy on the one hand, and the domain wall energy on the other, are identical in FMs and AFMs.

In the following we will focus on the simplest example

of a magnetic nanoparticle, which switches by coherent rotation between two stable magnetic states separated by an energy barrier ΔE . Thermal activation allows the nanoparticle's magnetic state to jump between states with a characteristic time scale. From the theory point of view, realistic models of such processes remains a considerable task. Simplifications rely often on the so-called single-domain approximation, where the total magnetization of the nanoparticle is described by a unique magnetic moment. Thermally activated dynamics can be calculated within the framework of the macroscopic stochastic Landau-Lifshitz-Gilbert [28, 29]

$$(1 + \alpha^2)\dot{\mathbf{m}} = -\gamma\mathbf{m} \times (\mathbf{h}_m + \alpha\mathbf{m} \times \mathbf{h}_m), \quad (1)$$

here, α is the damping constant, γ is the gyromagnetic ratio, \mathbf{m} the magnetization of the nanoparticle and $\mathbf{h}_m = -\delta_{\mathbf{m}}\mathcal{F} + \boldsymbol{\xi}$ the effective field, where \mathcal{F} is the magnetic free energy of the system and $\boldsymbol{\xi}$ are stochastic thermal fields as introduced by Brown [23]. For simplicity, in this work we restrain to an uniaxial particle, $\mathcal{F} = -H_a m_z^2/2m_0$, where H_a is the anisotropy field and m_0 the saturation magnetization. This free energy has two minima stable states, for example at $T = 0$ K, $m_z/m_0 = 1$ and $m_z/m_0 = -1$, with the energy barrier between them being $\Delta E = H_a m_0/2 = d_z N$, here N is the number of spins in the nanoparticle.

In the limit of low temperatures, $k_B T \ll \Delta E$, the reversal or switching time is fairly described by the exponential Néel-Arrhenius law $\tau = \tau_0 \exp(\Delta E/k_B T)$, where the prefactor τ_0 and the energy barrier ΔE depend on the mechanism of reversal [16]. For sufficiently small nanoparticles, coherent rotation over the energy barrier is the main mechanism, as sketched in Figure 1. For this mechanism analytical asymptotes for the reversal time were derived by Brown [23]

$$\tau_{\text{fm}} = \frac{1 + \alpha^2}{\alpha} \omega_a^{-1} \sqrt{\frac{\pi k_B T}{d_z N}} \exp(d_z N/k_B T). \quad (2)$$

The inverse of the prefactor of the e-function above is called attempt frequency. Its first factor is related to the damping dependence of the reversal time, clearly with a minimum at $\alpha = 1$. The second factor is the precessional time scale of the system, with $\omega_a = \gamma H_a = \gamma 2d_z/\mu_s$, where μ_s is the atomic magnetic moment. At finite temperatures, temperature dependent parameters need to be considered as pointed out by Nowak and co-workers [30].

For AFMs, to the best of our knowledge, an analytical asymptotes similar to Eq. (2) remains unknown. Only a few recent works have addressed the problem [19, 20]. However, they assumed AFM nanoparticles with uncompensated magnetic moments, which results in an effective ferromagnet with a very small magnetic moment. The completely compensated AFMs we will consider here are expected to behave qualitatively different. In order to estimate a similar asymptote for AFMs, we need an equa-

tion of motion for the AFMs including dissipative processes. While for FMs the Gilbert model for dissipation, Eq. (1), has been shown successful so far, the dissipative processes in AFMs are still a challenging problem.

Recent progress regarding the description of dissipative spin dynamics in AFMs can be summarized in the following equations of motion [31–34],

$$\dot{\mathbf{n}} = -\mathbf{n} \times (\gamma\mathbf{h}_m - \alpha_m \dot{\mathbf{m}}) - \mathbf{m} \times (\gamma\mathbf{h}_n - \alpha_n \dot{\mathbf{n}}) \quad (3)$$

$$\dot{\mathbf{m}} = -\mathbf{m} \times (\gamma\mathbf{h}_m - \alpha_m \dot{\mathbf{m}}) - \mathbf{n} \times (\gamma\mathbf{h}_n - \alpha_n \dot{\mathbf{n}}), \quad (4)$$

where α_m and α_n are related to the rate of power dissipation $P = \alpha_m \dot{\mathbf{m}}^2 + \alpha_n \dot{\mathbf{n}}^2$. The dynamics variables are here the magnetization $\mathbf{m} = (\mathbf{m}_1 + \mathbf{m}_2)/2$ and the Néel vector $\mathbf{n} = (\mathbf{m}_1 - \mathbf{m}_2)/2$. The effective fields are $\mathbf{h}_{m(n)} = -\delta_{\mathbf{m(n)}}\mathcal{F}$ where, for a generic antiferromagnet, the free energy reads $\mathcal{F} = H_e \mathbf{m}^2/2m_0 + \sum_{i=x,y,z} A(\partial_i \mathbf{n})^2 - H_a n_z^2/2m_0 - \mathbf{H} \cdot \mathbf{m}$, with $H_e = zJ/\mu_s$ being the homogeneous exchange field, z being the number of nearest neighbors and J the antiferromagnetic exchange constant, A the micromagnetic exchange stiffness, and $H_a = 2d_z/\mu_s$ the anisotropy field. In our case, the effective fields can be derived from a simplified free energy for mono-domain particles ($\sum_{i=x,y,z} A(\partial_i \mathbf{n})^2 = 0$) in absence of an external field, $\mathcal{F} = H_e \mathbf{m}^2/2m_0 - H_a n_z^2/2m_0$. In order to simplify, we keep terms up to linear order of \mathbf{m} in Eqs. (3) and (4) [32, 34]

$$\dot{\mathbf{n}} = -\mathbf{n} \times (\gamma\mathbf{h}_m - \alpha_m \dot{\mathbf{m}}) \quad (5)$$

$$\dot{\mathbf{m}} = -\mathbf{n} \times (\gamma\mathbf{h}_n - \alpha_n \dot{\mathbf{n}}). \quad (6)$$

By substituting Eq. (6) into (5) we obtain

$$\dot{\mathbf{n}} = -\gamma\mathbf{n} \times \mathbf{h}_m - \gamma\alpha_m \mathbf{n} \times \mathbf{n} \times \mathbf{h}_n. \quad (7)$$

While the value of α_n can be obtained from the decay of the small oscillations — the life-time of the excitation — of the Néel vector \mathbf{n} , $\alpha_n = \alpha\sqrt{H_e/H_a}$ [9], the value of α_m should come from the decay of the magnetization vector \mathbf{m} [35]. To estimate its value we consider only dissipation in the Gilbert sublattice equations (see Eq. (1)) $\dot{\mathbf{m}}_i = \gamma\alpha\mathbf{m}_i \times (\mathbf{m}_i \times (\mathbf{H}_a + \mathbf{H}_{\text{ex}}))$, and we also consider that the exchange field is usually larger than the anisotropy field, $H_a + H_e \approx H_a(H_e/H_a)$. Moreover, due to the symmetry of the exchange and anisotropy fields, \mathbf{h}_n acting in each sublattice is the same but staggered, thus one finds $\dot{\mathbf{n}} = \gamma\alpha_m \mathbf{n} \times (\mathbf{n} \times \mathbf{h}_n)$, with $\alpha_m = \alpha H_e/H_a$, which also implies $\alpha_m \gg \alpha_n$ [33]. Since typically $H_e \gg H_a$, the damping of the antiferromagnet is enhanced. To simplify the notation we define the small parameter $\epsilon = H_a/H_e = 2d_z/zJ$, so that $\alpha_m = \alpha/\epsilon$. This simple derivation can be extended to account for Gilbert-like damping, $\alpha_m = \alpha_{\text{afm}}/(1 + \alpha_{\text{afm}}^2)$.

The asymptotes of the reversal time in AFMs can be calculated similarly to FMs in Eq. (2). First of all, we note that, the energy barrier ΔE remains the same for both, FMs and AFMs, as long as all individual spin rotate coherently during switching (see Fig. 1). The

main differences regarding the spin dynamics in FMs and AFMs come from the typical eigen frequencies and the exchange-enhanced damping. In FMs, \mathbf{m} precesses around the anisotropy field H_a , while in AFMs, \mathbf{n} precesses around the exchange field $H_e \gg H_a$. For both, the damping is governed by the anisotropy field, but in case of the AFM, the damping parameter is exchange enhanced as stated before.

Under these assumptions and in analogy with the ferromagnetic case, we propose the following expression for the reversal time of an antiferromagnetic particle, which is the main result of our work,

$$\tau_{\text{afm}} = \frac{\epsilon^2 + \alpha^2}{\alpha} \omega_a^{-1} \sqrt{\frac{\pi k_B T}{d_z N}} \exp(d_z N / k_B T). \quad (8)$$

From this equation, we can directly see that the dependence of the reversal time as a function of the damping parameter α is clearly different for AFMs and FMs. In AFMs, it presents a minimum at $\alpha = \epsilon = 2d_z/zJ$, while in FMs at $\alpha = 1$. Interestingly, in AFMs this minimum depends on the ratio between the anisotropy and the exchange field, which will be material dependent.

To test the validity of Eq. (8) we performed computer simulations based on atomistic spin dynamics methods. Atomistic spin dynamics methods are a well-established numerical technique that allows to investigate the magnetization dynamics of magnetic nanoparticles. For the description of the magnetic system, we introduce the classical atomistic spin Hamiltonian

$$\mathcal{H} = -\frac{1}{2} \sum_{i,j} J_{ij} \mathbf{S}_i \mathbf{S}_j - \sum_i d_z (S_i^z)^2 \quad (9)$$

Here the \mathbf{S}_i variables denote unit vectors, J_{ij} is the Heisenberg exchange interaction between atoms at neighboring sites i and j . In this work we use only first nearest neighbors interaction, therefore $J_{ij} = J$. When $J > 0$, the ground state is ferromagnetic, while for $J < 0$ it is antiferromagnetic. d_z is the single-ion magneto-crystalline anisotropy at site i . The ground state of the system lies along the z -direction.

Atomistic spin dynamics are described by the Landau-Lifshitz-Gilbert equation,

$$(1 + \alpha_i^2) \mu_{s_i} \dot{\mathbf{S}}_i = -\gamma_i \mathbf{S}_i \times [\mathbf{H}_i + \alpha_i (\mathbf{S}_i \times \mathbf{H}_i)]. \quad (10)$$

By including a Langevin thermostat, the spin dynamics including statistical – equilibrium and non-equilibrium – thermodynamic properties can be obtained in the classical approximation. The effective local magnetic field on a lattice site, i , is

$$\mathbf{H}_i = -\frac{\partial \mathcal{H}}{\partial \mathbf{S}_i} + \boldsymbol{\xi}_i(t), \quad (11)$$

where $\boldsymbol{\xi}_i$ is a field-like stochastic process. Here we consider the white noise limit [36]

$$\langle \boldsymbol{\xi}_i(t) \rangle = 0, \quad \langle \boldsymbol{\xi}_{i,a}(0) \boldsymbol{\xi}_{j,b}(t) \rangle = \frac{2\alpha k_B T \mu_{s_i}}{\gamma_i} \delta_{ij} \delta_{ab} \delta(t), \quad (12)$$

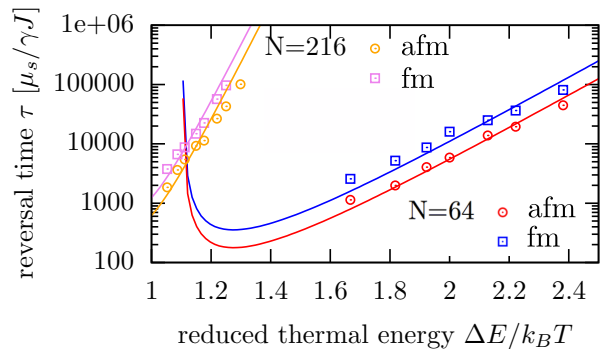


FIG. 2. Temperature dependence of the reversal time for two cubic nanoparticles composed of $N = 64$ and $N = 216$ spins, for ferromagnetic and antiferromagnetic ordering. Symbols correspond to simulations using atomistic spin model and lines to modified Brown's formula as described in the main text.

where a and b denote the Cartesian components.

We start by comparing the reversal time gained from numerical experiments to analytical expressions (Eqs. (2) and (8)) for small FM and AFM nanoparticles with the same anisotropy $d_z = 0.1 J$ (for AFM $\epsilon = 1/30$) and absolute value of the exchange interaction J . Here, we fix the damping parameter to $\alpha = 1$. Simulations were performed in cubic nanoparticles of two different sizes composed of $N = 4^3 = 64$ and $N = 6^3 = 216$ spins. For direct comparison between Brown's asymptotes and computer simulations based on atomistic spin dynamics, it has been demonstrated in FM nanoparticles that one needs to account for the temperature dependence of the magnetic parameters in Eq. (2) [30]. For example, the anisotropy field H_a is reduced as function of temperature and one can use the Callen-Callen theory with $H_a(T) = H_a m_e^3$, where m_e is the normalized equilibrium magnetization [37, 38]. For 3d Heisenberg spin models, the phenomenological relation $m_e = (1 - T/T_c)^{1/3}$ describes well computer simulation results for the temperature dependence of m_e [39]. Furthermore, we need to account for finite size effects. Computer simulations of thermal activation are very computation time consuming, thus, one can only perform simulations of nanoparticles of rather small size. Small systems have a reduced magnetization at a given temperature, as expected as a result of reduced coordination at the surfaces. For 3d Heisenberg spin models finite size scaling theory provides a value for the apparent Curie temperature as a function of the size L (linear characteristic length of the nanoparticle), $T_c(L)/T_c^\infty = 1 - (d_0/L)^{1/\nu}$, where the parameter d_0 correspond to characteristic exchange length, and ν to the critical exponent. A recent work in 3d Heisenberg spin model nanoparticles has estimated $d_0 = 0.4$ nm, and $\nu = 0.856$ [40], which we will use in the following.

Figure 2 shows results from numerical simulations (symbols) and Eqs. (2) and (8) (lines). First, we can ob-

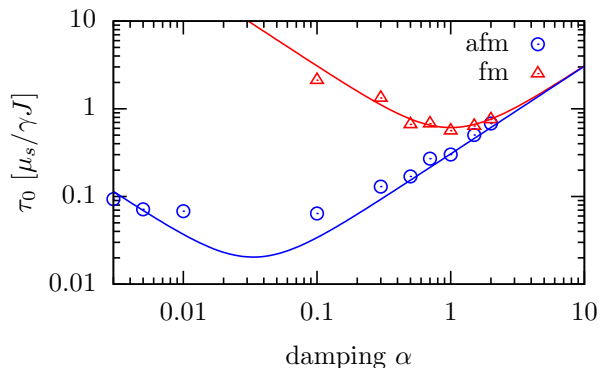


FIG. 3. Damping dependence of the reversal time for cubic nanoparticles ($N = 64$), for ferromagnetic and antiferromagnetic ordering. Symbols correspond to simulations using atomistic spin dynamics methods and lines to fitting function based in Eq. (2) and (8).

serve that the temperature dependence is correct and the same for FMs and AFMs, which means that the mechanism, coherent rotation, and the energy barrier ΔE are the same for both FMs and AFMs. The differences between AFM and FM come from the different damping term. In particular, one can easily estimate the ratio between reversal times in AFM and FM $\tau_{\text{fm}}/\tau_{\text{afm}} = \frac{1+\alpha^2}{\epsilon^2+\alpha^2}$, for $\alpha = 1$ we get $\tau_{\text{fm}}/\tau_{\text{afm}} \approx 2$. Along this line, in order to validate the damping dependence of the reversal time in both FMs and AFMs, we perform computer simulations by varying the damping value α . This is interesting since Eq. (8) predicts strong differences at relatively low damping $\alpha \ll 1$. Figure 3 shows the so-called inverse attempt frequency $\tau_0 = \tau/\exp(\Delta E/k_B T)$ as a function of damping for AFMs and FMs. Symbols correspond to simulations of the reversal time divided by $\exp(\Delta E/k_B T)$, analytical lines correspond to Eq. (8) divided by $\exp(\Delta E/k_B T)$, where $\Delta E = 5$ J. Here, we can see that for typical values of intrinsic damping in magnetic materials, $\alpha = 0.001-0.01$ (0.0025 for Mn_2Au [41]), the reversal time of AMFs could be up to several orders of magnitude shorter than in FMs, which effectively means much less thermal stability.

In FMs, one solution to the problem of reduced thermal stability for ever decreasing nanoparticle volumes is an increase of the magnetic anisotropy. Therefore, we investigate finally the dependence of the reversal time as a function of the anisotropy d_z . As discussed above, since the reversal time in AFMs strongly depends on $\epsilon \sim d_z/J$, one could engineer nanoparticle parameters to maximize thermal stability in AFMs. To validate our predictions, we use atomistic spin dynamics to perform simulation of nanoparticles composed of $N = 64$ spins for two different anisotropy parameters, $d_z = 0.1$ J and 0.01 J. We fix the damping parameter to $\alpha = 0.3$. One can observe in Figure 4 that the results coming out from computer simulations agree very well with our theoretical predictions.

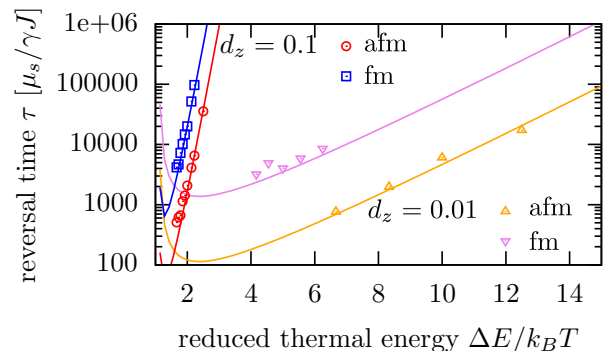


FIG. 4. Anisotropy dependence of the reversal time for cubic nanoparticles ($N = 64$), for ferromagnetic and antiferromagnetic ordering. Symbols correspond to simulations using atomistic spin dynamics methods and lines to fitting function based in Eq. (2) and (8).

As predicted, the ratio $\tau_{\text{fm}}/\tau_{\text{afm}}$ is larger for $d_z = 0.01$ J than for $d_z = 0.1$ J. We predict that AFM nanoparticles present much faster thermally activated reversal dynamics, which restrains their potential use as active elements in nanoscale devices. Our results predict that the role of the magnetic anisotropy in the thermal stability of AFM nanoparticles is dramatic. Relatively high anisotropy values will lead to a similar thermal stability than FMs. For $\epsilon \gg \alpha$ (usually $\alpha = 0.01-0.001$) the ratio $\tau_{\text{fm}}/\tau_{\text{afm}} = \frac{1+\alpha^2}{\epsilon^2+\alpha^2} \rightarrow 1/\epsilon^2 = (zJ/2d_z)^2$.

In summary, we investigated the superparamagnetic limit of antiferromagnetic nanoparticles analytically as well as by means of computer simulations. We find a drastically reduced thermal stability because of the exchange enhancement of the attempt frequencies and the effective damping during the antiferromagnetic switching process. For realistic materials, the reversal times of AFMs can be expected to be four to five orders of magnitude shorter than that of FMs, a finding that is in agreement with a work on antiferromagnetic grains in exchange bias systems [42]. These findings limit the potential of scaling down AFM nanostructures and have a direct implication on the design of new antiferromagnetic spintronic devices.

Financial support for this work at Konstanz University was provided by the Deutsche Forschungsgemeinschaft via SFB 1214 and the Priority Program SpinCaT. At the FU Berlin support by the Deutsche Forschungsgemeinschaft through SFB/TRR 227 "Ultrafast Spin Dynamics", Project A08 is gratefully acknowledged.

* unai.atxitia@fu-berlin.de

- [1] B. G. Park et al., Nat. Mater. **10**, 347 (2011).
- [2] T. Jungwirth, X. Marti, P. Wadley, and J. Wunderlich, Nat. Nanotech. **11**, 231 (2016).

- [3] P. Wadley et al. *Science* **351**, 587 (2016).
- [4] K. Olejnik, et al. *Sci. Adv.* **4** eaar3566 (2018).
- [5] V. Baltz, A. Manchon, M. Tsoi, T. Moriyama, T. Ono, and Y. Tserkovnyak *Rev. Mod. Phys.* **90**, 015005 (2018).
- [6] T. Jungwirth, et al. *Nat. Physics* **14**, 200 (2018).
- [7] O. V. Gomonay and V.M. Loktev *Low Temperature Physics*, **40**, 17 (2014).
- [8] S. Selzer, U. Atxitia, U. Ritzmann, D. Hinzke, and U. Nowak, *Phys. Rev. Lett.* **117**, 107201 (2016).
- [9] O. Gomonay, T. Jungwirth, and J. Sinova *Phys. Rev. Lett.* **117**, 017202 (2016).
- [10] N. Thielemann-Kühn, D. Schick, N. Pontius, C. Trabant, R. Mitzner, K. Holldack, H. Zabel, A. Föhlisch, and C. Schüfller-Langeheine, *Phys. Rev. Lett.* **119**, 197202 (2017).
- [11] W. Wernsdorfer, E. B. Orozco, K. Hasselbach, A. Benoit, B. Barbara, N. Demoncy, A. Loiseau, H. Pascard, and D. Mailly, *Phys. Rev. Lett.* **78**, 1791 (1997).
- [12] M. Bode, O. Pietzsch, A. Kubetzka, and R. Wiesendanger, *Phys. Rev. Lett.* **92**, 067201 (2004).
- [13] D. A. Garanin, *Phys. Rev. B* **78**, 144413 (2008).
- [14] W. T. Coffey and Yu. P. Kalmykov, *Journal of Applied Physics* **112**, 121301 (2012).
- [15] A. Balan, P. M. Derlet, A. F. Rodríguez, J. Bansmann, R. Yanes, U. Nowak, A. Kleibert, and F. Nolting, *Phys. Rev. Lett.* **112**, 107201 (2014).
- [16] Yu. P. Kalmykov and W. T. Coffey, *Brownian Motion of Classical Spins: Application to Magnetization Relaxation in Nanomagnets in The Langevin Equation: 4th*, pp. 495-670 (2017).
- [17] A. Kleibert, A. Balan, R. Yanes, P. M. Derlet, C. A. F. Vaz, M. Timm, A. Fraile Rodríguez, A. Béché, J. Verbeeck, R. S. Dhaka, M. Radovic, U. Nowak, and F. Nolting, *Phys. Rev. B* **95**, 195404 (2017).
- [18] V. Skumryev, S. Stoyanov, Y. Zhang, G. Hadjipanayis, D. Givord, and J. Nogués, *Nature* **423**, 850 (2003).
- [19] Yu. L. Raikher and V. I. Stepanov, *Zh. Eksp. Teor. Fiz.* **134**, 514 (2008), [*J. Exp. Theor. Phys.* **107**, 435 (2008)].
- [20] B. Ouari, S. Aktaou, and Yu. P. Kalmykov, *Phys. Rev. B* **81**, 024412 (2010).
- [21] S. Loth, S. Baumann, C. P. Lutz, D. M. Eigler, and A. J. Heinrich, *Science* **335**, 196 (2012).
- [22] D. Hinzke and U. Nowak, *J. Magn. Magn. Mat.* **221**, 365 (2000).
- [23] W. F. Brown, Jr., *Phys. Rev.* **130**, 1677 (1963).
- [24] H. B. Braun, *Phys. Rev. Lett.* **71**, 3557 (1993).
- [25] H. B. Braun, *Stochastic magnetization dynamics in magnetic nanostructures: from Néel-Brown to soliton-antisoliton creation in Structure and Dynamics of Heterogenous Systems*, edited by P. Entel and D. E. Wolf (World Scientific, Singapore, 2000).
- [26] D. Hinzke and U. Nowak, *Phys. Rev. B* **58**, 265 (1998).
- [27] D. Hinzke and U. Nowak, *Phys. Rev. B* **61**, 6734 (2000).
- [28] L. Landau and E. Lifshitz, *Phys. Zeitsch. der Sow.* **8**, 153 (1935).
- [29] T. L. Gilbert, *Phys. Rev.* **100** 1243 (1955); T. L. Gilbert, *IEEE Trans. Magn.* **40**, 3443 (2004).
- [30] U. Nowak, O. N. Mryasov, R. Wieser, K. Guslienko, and R. W. Chantrell, *Phys. Rev. B* **72**, 172410 (2005).
- [31] O. V. Gomonay and V. M. Loktev *Low Temperature Physics*, **34**, 198 (2008).
- [32] K. M. D. Hals, Y. Tserkovnyak, and A. Brataas, *Phys. Rev. Lett.* **106**, 107206 (2011).
- [33] Q. Liu, H. Y. Yuan, K. Xia, and Z. Yuan, *Phys. Rev. Materials* **1**, 061401(R) (2017).
- [34] H. Y. Yuan et al., arXiv:1801.00217 (2018).
- [35] A. G. Gurevich and G. A. Melkov, *Magnetization oscillations and waves*, (CRC Press, 1996).
- [36] U. Nowak, *Classical spin models in Handbook of Magnetism and Advanced Magnetic Materials* edited by H. Kronmüller and S. Parkin (Wiley, 2007).
- [37] H. B. Callen, *Phys. Rev.* **130**, 890 (1963).
- [38] H. B. Callen and E. Callen, *J. Phys. Chem. Sol.* **27**, 1271 (1966).
- [39] R. F. L. Evans, U. Atxitia, and R. W. Chantrell, *Phys. Rev. B* **91**, 144425 (2015).
- [40] M. O. A. Ellis and R. W. Chantrell, *Appl. Phys. Lett.* **106** 162407 (2015)
- [41] N. Bhattacharjee et al., arXiv:1802.03199 (2018).
- [42] G. Vallejo-Fernandez, N. P. Aley, J. N. Chapman, and K. O'Grady, *Appl. Phys. Lett.* **97**, 222505 (2010).